



## **Kinetic and thermodynamic studies on adsorption of copper (II) ions onto the olive pomace lignocellulosic in the region of Beni Mellal (MOROCCO)**

**A. Menichi<sup>\*</sup>, A. Chagraoui, N. Nadi, A. Moussaoui, A. Tairi, O. Ait Sidi Ahmed, L. Loubbidi, L. Bourja**

*Laboratory of Physical-Chemistry of Applied Materials (LPCMA), Faculty of Science Ben M'sik, University Hassan II-Casablanca (Morocco).*

<sup>\*</sup>Corresponding Author. E-mail: [menichi.aziz@gmail.com](mailto:menichi.aziz@gmail.com)

### **Abstract**

The aim of the present work is the valorization of lignocellulosic material prepared from olive pomace in the field of pollutant treatment of various liquid effluents containing heavy metals toxics such as copper. The chemical characterization of the surface was carried out by the pH at the point of zero charge, this indicates the acidic character of the materials. The satisfactory operating conditions were performed at pH 4, a particle size below 80  $\mu\text{m}$  and a temperature of 20°C. The characterization of solids obtained before and after elimination of the hemicellulose of the olive pomace was performed by Infrared Spectroscopy and Scanning Electron Microscopy. The results showed that the elimination of hemicellulose has a great influence on the structural and morphological properties as well as the cation exchange capacity of olive pomace. The kinetic study (pseudo-first order and pseudo-second-order), thermodynamic and mechanistic (isotherms Langmuir, Freundlich, Temkin and Dubinin Radushkevich) of the adsorption of Cu(II) ions on the lignocellulosic obtained from the olive pomace was conducted in aqueous solution. The results gotten have permeated us to specify in a static reactor: the sorption kinetics and the thermodynamic parameters of sorption of copper ions.

*Keywords:* lignocellulosic, liquid effluents, heavy metal, hemicellulose, kinetic, isotherm.

### **Introduction**

Filtration, adsorption, reverse osmosis, solvent extraction, and membrane separation techniques are used for removal of heavy metals in aqueous solution, the chemical precipitation is a conventional technique. Adsorption has been shown to be an economically feasible alternative method for removing heavy metals from wastewater and water supplies [1,2]. Indeed, adsorption of metal on materials considered as a waste of natural origin is the most important chemical process, affecting their behavior and bioavailability [3]. This technique can be controlled by physical attraction, the chemical bonds of complexation with surface functional groups, or formation of hydrate on the surface [4,5]. Also, its use is wide enough because it is easy to apply it [6].

In addition, heavy metals have negative effects on all environmental compartments, it is important to balance these elements with precision to ensure that standards are met. Otherwise, it is essential to use pollution control processes to eliminate them [7]. Copper may cause irritation by inhalation, allergy in contact and liver damage if it is taken orally over a long period. It has the distinction of being somewhat toxic to humans but highly toxic to aquatic plants. It is therefore important to limit the concentration in the surface water [8]. And international regulations impose a maximum content of 1mg/l of copper [9].

This work is devoted to removal by adsorption of copper(II) onto the lignocellulosic olive pomace (LCOP) extracted from crude olive pomace (COP) in the region of Beni Mellal. The adsorption kinetic in a static reactor using equations of pseudo-first, pseudo-second order and thermodynamic modeling of copper retention in different temperatures to determine various parameters of equilibrium: the maximum adsorption capacity, the energy of adsorption and the constants of equilibrium adsorbate-adsorbent has been highlighted.

## 2. Materials and methods

### 2.1. Solutions and reagents

The elimination of hemicellulose is an important part to obtain (LCOP). In a flask of 250ml, a dry mass of 20g pretreated fiber is mixed with 100ml of distilled water. The mixture is brought to reflux under continuous stirring for 2h at 80°C and then vacuum filtered; the filtrate obtained contains hemicelluloses while the residue contains cellulose, lignin and other compounds. After that, the residue was dried at a temperature of 110°C for 24h in an oven; the material is then crushed and sieved to obtain a series of samples with a size of between 80µm and 2mm.

All experiments were performed in batch reactors (static system) with solutions of CuSO<sub>4</sub>.5H<sub>2</sub>O at well defined concentrations and temperature. The dosage of copper Cu(II) is carried out by complexometric EDTA (disodium salt) in the presence of murexide as an indicator [10].

### 2.2. Determination of pH of zero charge

The pH at the point of zero charge (pH<sub>PZC</sub>) is defined as the pH of the aqueous solution in which the solid is in a neutral electric potential [11].

Solutions of 0.01M of NaCl with a pH between 2 and 12 (adjusted by adding an aqueous solution of NaOH or of 0.1M HCl) were first prepared. 0.15g of dry (LCOP) is contacted with 50ml of each solution contained in glass-stoppered flasks. The suspensions are stirred for 48h at room temperature. Each solution is then filtered using a filter paper. After that, a new pH measurement is performed. The final pH curve is plotted= f(initial pH). PH<sub>PZC</sub> corresponds to the pH of the solution for which the curve passes through the first bisector (final pH = initial pH).

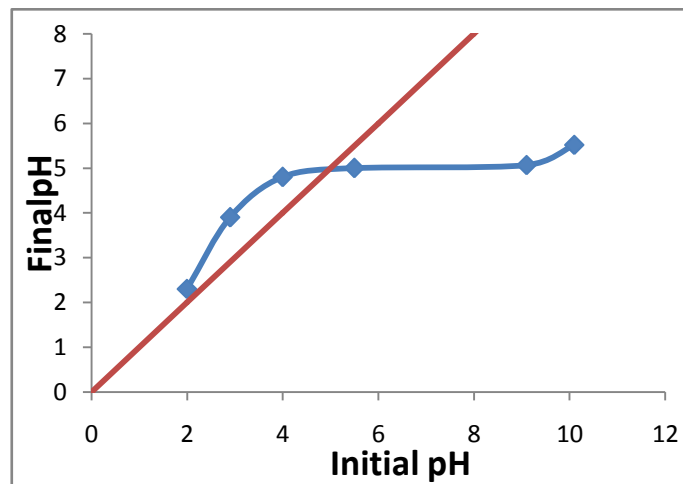
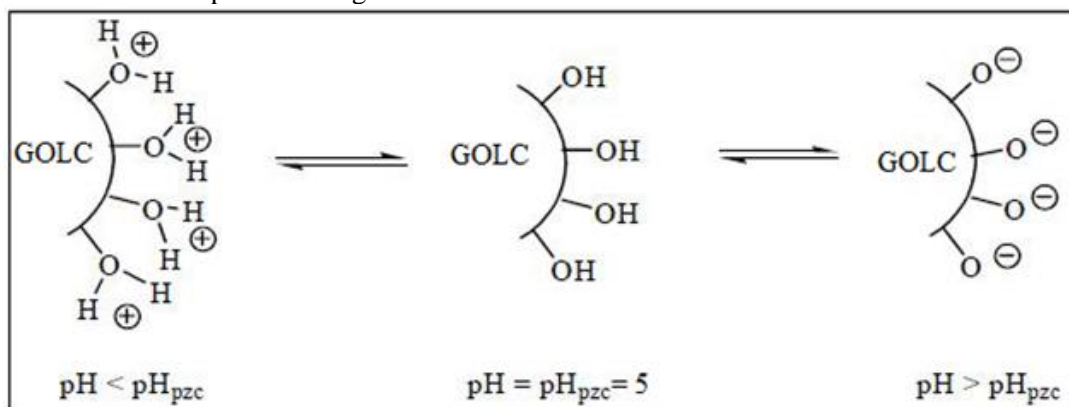


**Figure 1:** Determination of pH<sub>PZC</sub> of LCOP

The pH<sub>PZC</sub> of (LCOP) is 5. The solutions with a pH value below 5, the overall surface charge is positive while it is negative for those whose pH value is greater than 5.



The most probable retentions are a type of complexation of the Cu<sup>2+</sup> ions by its associates with the functional groups (OH, CO) that behave as complexing ligands in the chains of polymers [12].

### 2.3. Influence of pH on the adsorption of Cu (II)

The influence of initial solution pH on the adsorption was studied in the range of pH=2 to pH=5, by which there is no precipitation of Cu(II).

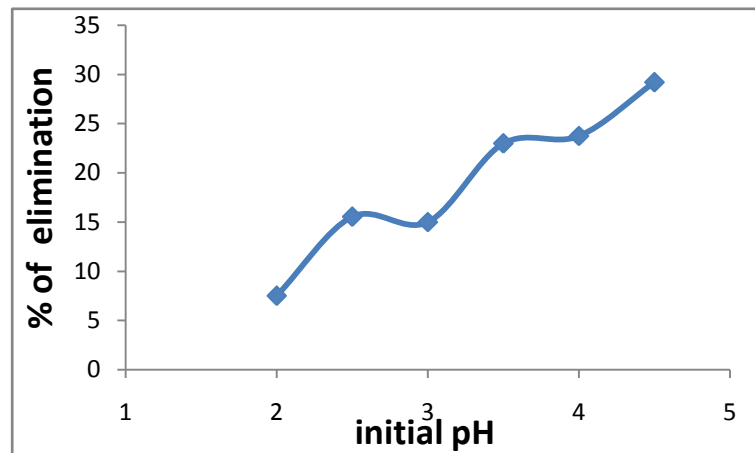


**Figure 2:** Effect of pH solutions on adsorption of Cu(II) on (LCOP)  $C_0=200\text{mg/l}$ ,  $m=1\text{g/l}$ ,  $T=20^\circ\text{C}$ ,  $\text{size}\leq 80\mu\text{m}$ , stirring rate =250t/min

It is found that there is a close relationship between the initial pH of the solution and the retention capacity of the Cu(II) by the adsorbent, the figure 2 shows that the capacity of adsorption increases proportionally with increasing pH of the solutions until reaching its maximum at pH=4.6 with an adsorption rate of 30%.

## 3. Resultats and discussion

### 3.1. Characterization of (COP) and (LCGO)

#### 3.1.1. Fourier Transform Infrared Spectroscopy

The infrared spectrum of the samples in figure 3.1 and figure 3.2 were recorded between 400 and  $4000\text{cm}^{-1}$  using a VERTEX 70 Fourier Transform Infrared Spectrometer.

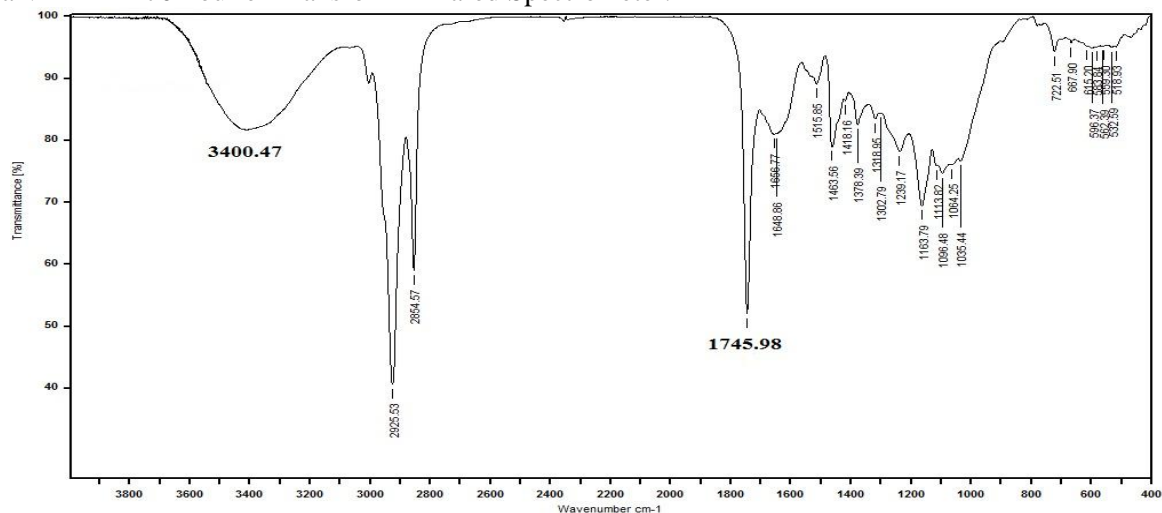


**Figure 3.1:** Infrared spectrum of the (COP)

Gaballah Kibertus [13] have suggested that the retention of Cu(II) by the wood is done by several mechanisms: reaction between Cu(II) and the carboxylic groups of the surface (RCOOH), by hydrogen bonds of hydrated  $\text{Cu}(\text{H}_2\text{O})_6$  with the cellulose; and the formation of complexes with the hydroxyl groups of the lignin surface.

The results of the FT-IR analysis revealed an appreciable increase in the intensity of the hydroxyl groups ( $3400\text{cm}^{-1}$ ) after the elimination of hemicellulose, and the disappearance of the peaks at  $1745\text{cm}^{-1}$  approximately is probably related to the decarboxylation of the surface, this confirms that the hemicellulose can prevent the adsorption of the Cu(II).

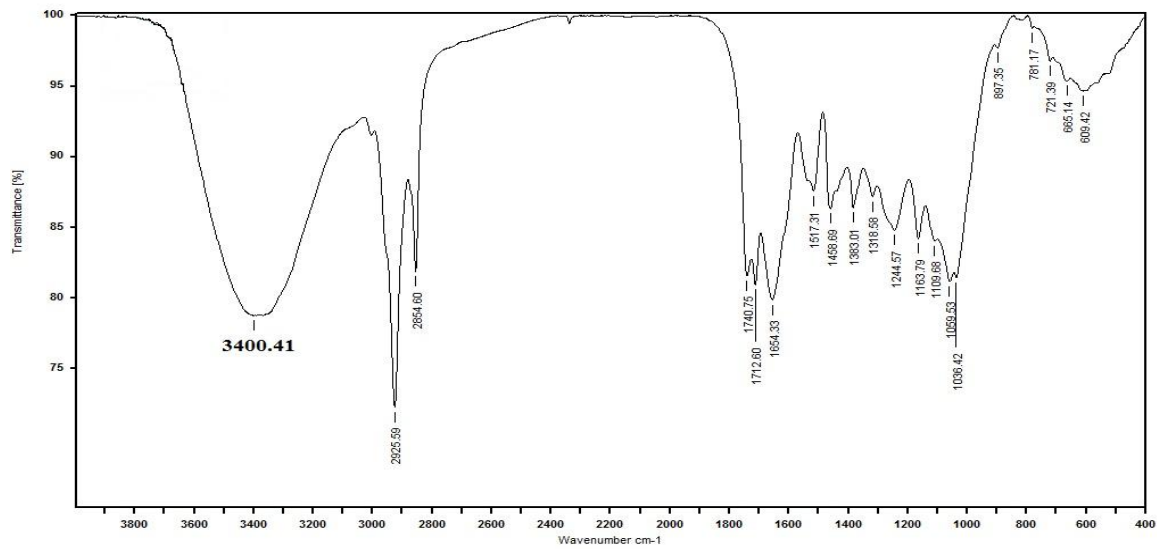


Figure 3.2: Infrared spectrum of the (LCOP)

### 3.1.2. Scanning Electron Microscopy SEM

The observation of each sample of olive pomace by the scanning electron microscope was carried out to observe the morphology of the grains. Two SEM images are taken at two different magnifications (Fig4.1, Fig4.2), the analysis of the photographs show that the (LCOP) presents a very heterogeneous porous structure comparing with the (OPC).

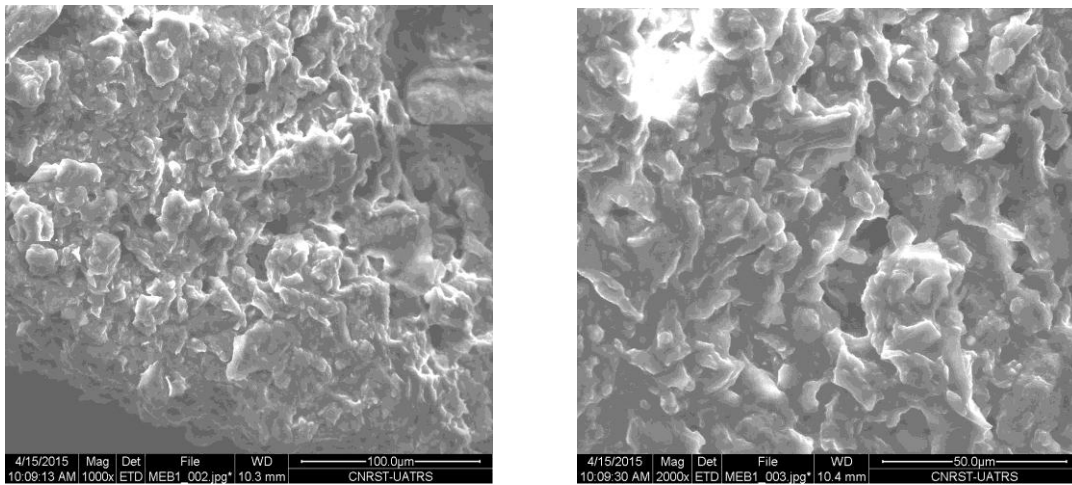


Figure 4.1: SEM images (OPC)

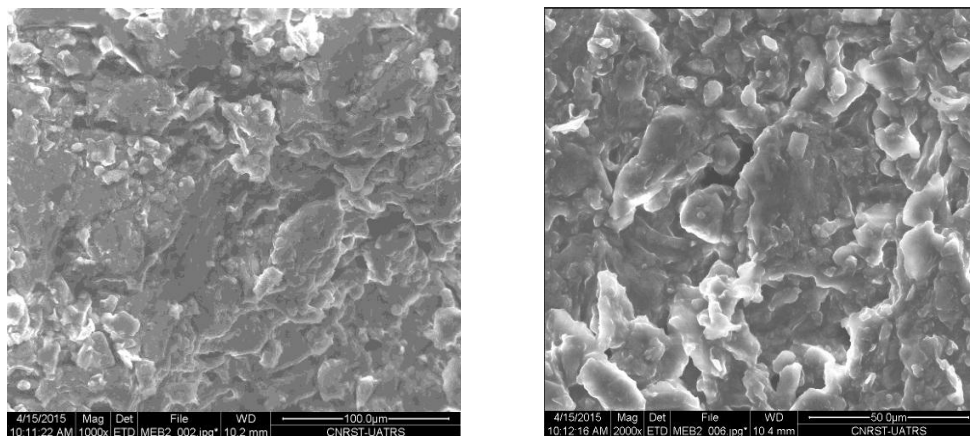


Figure 4.2: SEM images (LCOP)

### 3.2. Modeling of adsorption isotherms

#### 3.2.1. Adsorption Typology

The measurement of the equilibrium concentrations of the Cu(II) at different temperatures (25°C, 35°C and 45°C) allowed establishing the curves of adsorption isotherms.

The form of these isotherms can suggest the type of interaction between the adsorbate and the adsorbent. According to Gilles [14], there are four types: C-type, L-type, H-type and S-type.

The results obtained are shown in Figure 5:

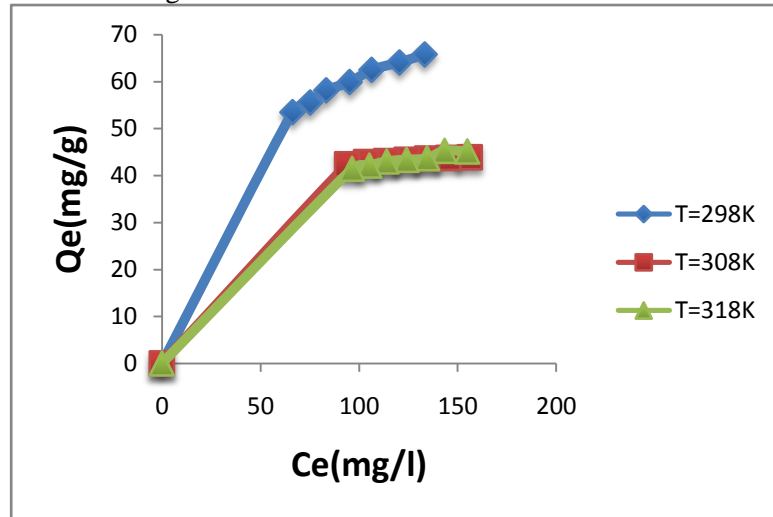


**Figure 5:** Isotherm of adsorption of Cu(II) on (LCOP)  
 $1.5 \leq m(\text{g/l}) \leq 2.5$ ,  $C_0=200\text{mg/l}$ , stirring rate= $250\text{t/min}$ ,  $\text{pH}=4$ , size $\leq 80\mu\text{m}$

The form of the adsorption isotherms of Cu(II) on the (GOLC) showed that the isotherm is L-type according to the classification of Gilles which implies the possibility to apply linear models of Langmuir, Freundlich, Temkin and Dubinin Radushkevich. The negative effect of adsorption at high temperature (35°C and 45°C) suggests that we have an exothermic adsorption phenomenon.

#### 3.2.2. Modeling of adsorption isotherms

a) The Langmuir model [15]

$$Q_e = \frac{K_L Q_m C_e}{1 + K_L C_e} \quad \text{linearizable in} \quad \frac{1}{Q_e} = \frac{1}{Q_m} + \frac{1}{Q_m K_L} \cdot \frac{1}{C_e}$$

Where **Qm**: maximum capacity of adsorption (mg/g); **K<sub>L</sub>**: is adsorption equilibrium constant of Langmuir isotherm (l/mg) ; Qm and K<sub>L</sub> can be determined by plotting 1/Q<sub>e</sub> vs 1/C<sub>e</sub>

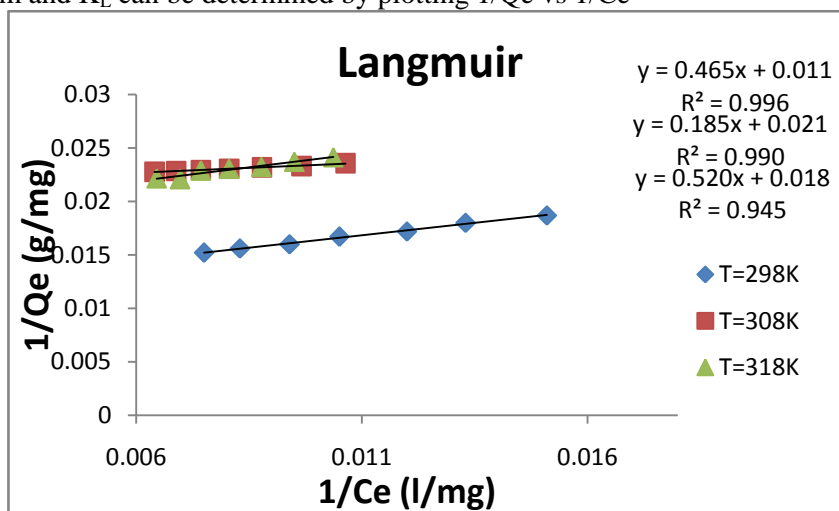


**Figure 6 :** Modeling of adsorption isotherms by the Langmuir equation  
 $1.5 \leq m(\text{g/l}) \leq 2.5$ ,  $C_0=200\text{mg/l}$ ,  $\text{pH}=4$ , stirring rate= $250\text{t/min}$ , stirring time= $1\text{h}$  and size $\leq 80\mu\text{m}$

According to the correlation coefficients, it is found that the adsorption isotherms of Cu(II) are well described by the Langmuir model. These results indicate that the adsorption is carried out with formation of a molecular monolayer, without interaction between the adsorbed molecules with a maximum adsorption capacity of about 85.5mg/g.

b) The Freundlich Model [16]

$$Q_e = K_F \cdot C_e^{\frac{1}{n}} \quad \text{Linearizable in} \quad \ln Q_e = \ln K_F + \frac{1}{n} \ln C_e$$

$K_F$  et  $1/n$  : is constant of Freundlich representing respectively the capacity and the intensity adsorption.

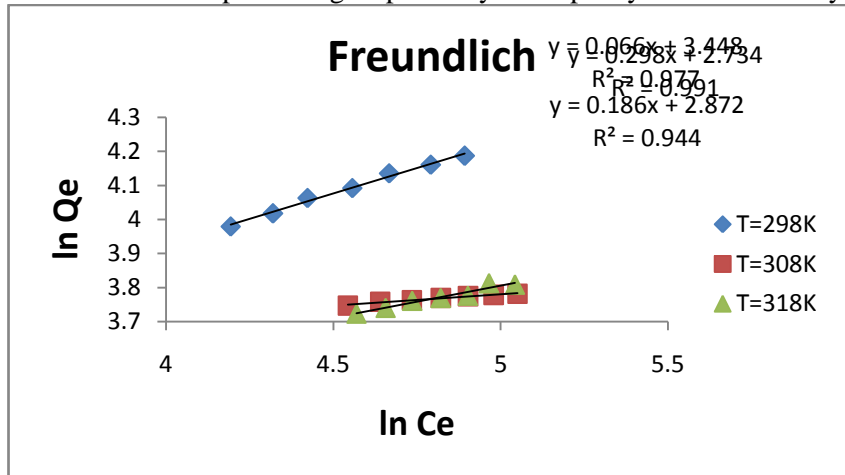


**Figure 7:** Modeling of adsorption isotherms by the Freundlich equation

$1.5 \leq m(\text{g/l}) \leq 2.5$ ,  $C_0=200\text{mg/l}$ ,  $\text{pH}=4$ , stirring rate= $250\text{t/min}$ , stirring time= $1\text{h}$  and size  $\leq 80\mu\text{m}$

The curves  $\ln Q_e = f(C_e)$  have led to the values of  $K_F$  and  $1/n$ . These values vary from one temperature to another. In fact,  $1/n$  is between 0 and 0.5 for all temperatures. This shows that the (LCOP) has a good affinity to adsorb Cu(II).

c) The Temkin Model [17]

The Temkin model transposed to the liquid phase [18,19,20]:

$$\frac{Q_e}{Q_m} = \theta = \left(\frac{RT}{\Delta Q}\right) \ln(K_T \cdot C_e) \quad \text{Linearizable in} \quad Q_e = \left[Q_m \left(\frac{RT}{\Delta Q}\right)\right] \cdot \ln C_e + \left[Q_m \left(\frac{RT}{\Delta Q}\right)\right] \cdot \ln K_T$$

$\theta$  : Recovery rate of the surface of the adsorbent ( $\text{kJ}\cdot\text{mol}^{-1}$ ) ;  $\Delta Q$  : the variation of adsorption energy ( $\text{kJ}\cdot\text{mol}^{-1}$ ),

$K_T$ : equilibrium constant and  $R=8.314 \text{ J}\cdot\text{mol}^{-1}\cdot\text{K}^{-1}$  constant of ideal gas.

$K_T$  and  $\Delta Q$  can be determined by plotting  $Q_e$  vs  $\ln C_e$ .

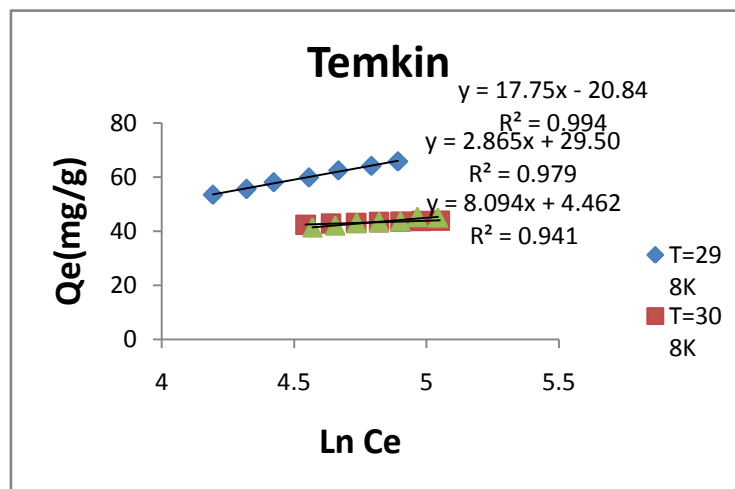


**Figure 8:** Modeling of adsorption isotherms by the Temkin equation

$1.5 \leq m(\text{g/l}) \leq 2.5$ ,  $C_0=200\text{mg/l}$ ,  $\text{pH}=4$ , stirring rate =  $250\text{t/min}$ , stirring time= $1\text{h}$  et size  $\leq 80\mu\text{m}$

The most important result that can be taken by applying the Temkin model is that the variation of the energy of adsorption increases with the temperature, this confirms that the reaction of adsorption is exothermic.

d) The Dubinin Radushkevich model [21]

$$Q_e = Q_m \exp(-\beta \varepsilon^2) \text{ Linearisable in } \ln Q_e = \ln Q_m - \beta \varepsilon^2$$

$\varepsilon$  : the potential of Polanyi, corresponding to:  $\varepsilon = RT \ln (1 + (\frac{1}{C_e}))$

$\beta$  : the constant adsorption per molecule of the adsorbate when it is transferred to the surface of the solid from infinity in the solution [22].  $\beta$  et  $E$  (kJ.mol<sup>-1</sup>) are linked by the relationship

$$E = \frac{1}{\sqrt{2\beta}}$$

By plotting  $\ln Q_e$  in function of  $\varepsilon^2$ , it is possible to get the value of  $Q_m$  (mol.g<sup>-1</sup>) and  $\beta$ .

$E$  can give an idea about the type of adsorption. If  $E$  is between 8 and 16 kJ mol<sup>-1</sup>, the process follows adsorption by ion exchange, whereas for values of  $E < 8$  kJ.mol<sup>-1</sup>, the adsorption process is the physical nature and if  $E > 16$  kJ.mol<sup>-1</sup> the process is dominated by diffusion intraparticle [23].

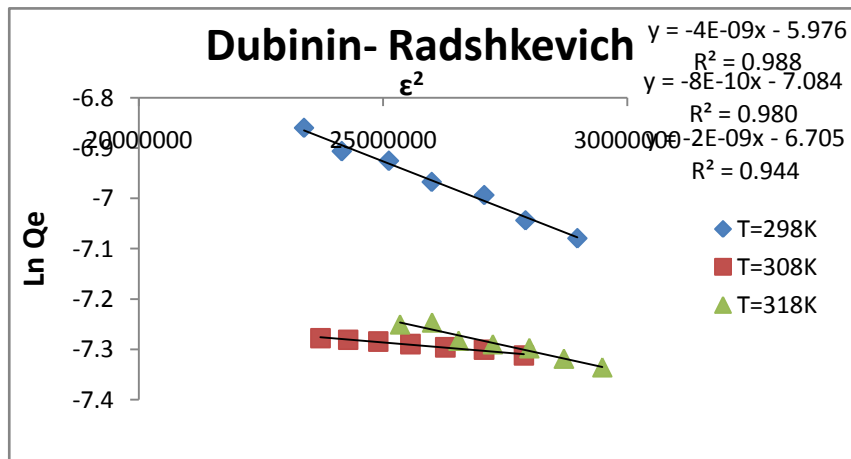


**Figure 9:** Modeling of adsorption isotherms by the Dubinin Radushkevich equation  $1.5 \leq m(g/l) \leq 2.5$ ,  $C_0=200mg/l$ ,  $pH=4$ , stirring rate=250t/min, stirring time=1h and size  $\leq 80\mu m$

The values of correlation coefficients  $R^2$  are around 0.99 and the calculated values of  $Q_e$  are very close to the experimental values for the pseudo second order model showing that this model is applied correctly and confirms chemisorptions of Cu (II) on the (LCOP).

The parameter values of Freundlich, Langmuir, Temkin and Dubinin-Radushkevich are summarized in Table1.

**Table1:** Parameters of adsorption models for different concentrations

T (°C)	Langmuir			Freundlich				Temkin			Dubinin Radushkevich		
	R <sup>2</sup>	Q <sub>m</sub>	KL.10-2	R <sup>2</sup>	Q <sub>m</sub>	K <sub>F</sub>	1/n	R <sup>2</sup>	ΔQ	KT	E	Q <sub>m</sub>	R <sup>2</sup>
25	0.996	85.5	2.51	0.992	76.7	15.4	0.298	0.995	11.9	0.309	11.2	161.3	0.989
35	0.938	57.8	2.94	0.950	52.3	15.7	0.227	0.943	14.5	0.674	25.0	53.3	0.980
45	0.945	53.2	3.61	0.944	47.6	17.7	0.187	0.942	17.4	1.736	15.8	77.8	0.944

### 3.3. Adsorption kinetics

#### 3.3.1. Pseudo first order model [24]

The Rate Law for the Adsorption:

$$\frac{dQ_e}{dt} = K_1 \cdot (Q_e - Q_t)$$

Integration of the model equations that we have used is constructed as follows

$$\ln(Q_t - Q_e) = \ln Q_e - K_1 \cdot t$$

$K_1$ : rate constant for a first-order reaction kinetics;  $Q_t$  : the capacity of adsorption at time t.  
 Linear representation of  $\ln(Q_e - Q_t)$  versus time allowed to determine the theoretical value of  $Q_e$  and the rate constant  $K_1$ .

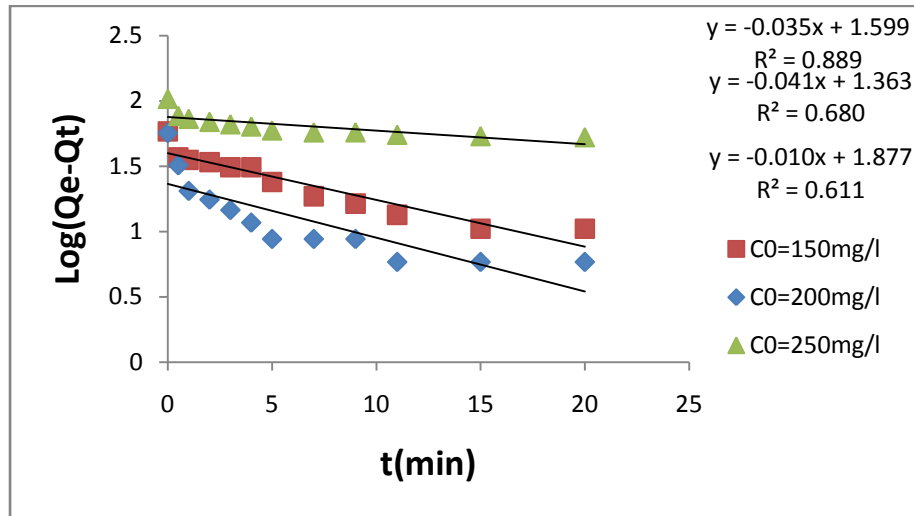


**Figure 10: Model-first order kinetics**  
 m=1g/l, stirring rate=250t/min, T=25°C and size≤ 80µm

### 3.3.2. Pseudo second order model [25]

Pseudo second order model is represented as follows:

$$\frac{dQ_e}{dt} = K_1 \cdot (Q_e - Q_t)^2$$

$K_2$  : rate constant for a second-order reaction kinetics

The integration of this equation gives:

$$\frac{t}{Q_t} = \frac{t}{Q_e} + \frac{1}{K_2 \cdot Q_e^2}$$

The linear representation of  $t/Q_t$  vs. t illustrated in (Fig.11) is used to determine the theoretical values of  $Q_e$  of the second order and the  $K_2$ .

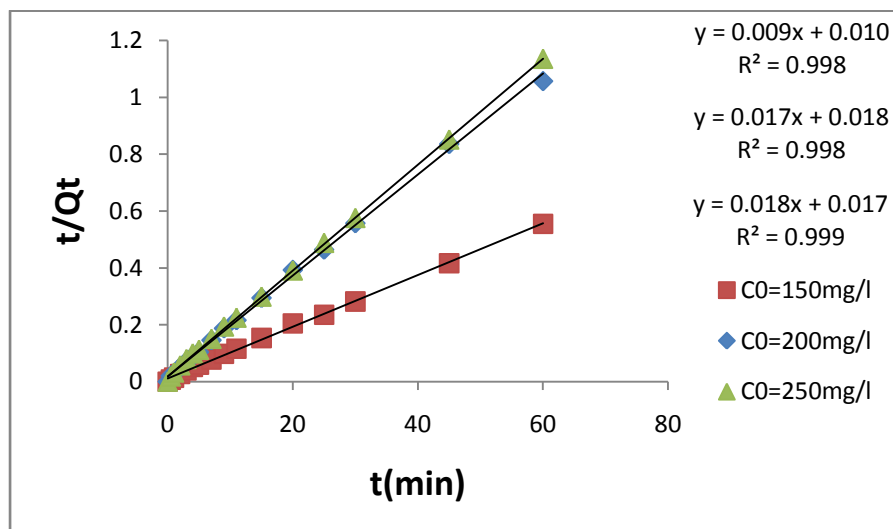


**Figure 11: Model-second order kinetics**  
 m=1g/l, stirring rate =250t/min, T=25°C and size≤ 80µm

The values of correlation coefficients  $R^2$  are around 0.99 and the calculated values of  $Q_e$  are very close to the experimental values for the pseudo second order model showing that this model is applied correctly and confirms chemisorptions of Cu (II) on the (LCOP).

**Table 2:** the parameters for the pseudo 1<sup>st</sup> order and 2<sup>nd</sup>-order kinetic model for the adsorption of Cu (II) on (LCOP).

	C <sub>0</sub> (mg/l)	Q <sub>e</sub> (calc) (mg/g)	Q <sub>e</sub> (exp)	K	R <sup>2</sup>
<b>1<sup>st</sup> order kinetic model</b>	150	39.73	58.2	0.036	0.8899
	200	23.12	56.8	0.041	0.6801
	250	75.35	52.87	0.011	0.7933
<b>2<sup>nd</sup> kinetic model</b>	150	109.89	58.2	0.009	0.9985
	200	56.2	56.8	0.017	0.9985
	250	53.76	52.87	0.019	0.9978

## Conclusion

The present study shows that (GOLC) has an acid character on its surface and that the adsorption capacity increases with the pH. Infrared spectra of the (GOB) and (GOLC) in the region of  $\nu_{OH}$  shows that elimination of the hemicellulose entail an increase of the total amount of hydroxyl group, probably due to the release of the hydrogen bonding between the cellulose and hemicellulose (GOLC). Moreover, the SEM analysis indicates that the (GOLC) has a porous and highly heterogeneous structure by comparing with (GOB).

The adsorption of Cu(II) ions on the (GOLC) is favored at room temperature and it checks the by model Langmuir, Freundlich, Temkin and Dubinin-Redushkevich, such ions are adsorbed monolayer without interaction between them, with a maximum capacity of 85.5mg / g, according to a chemisorption reaction with an exothermic effect. The kinetic study shows that the adsorption process is very fast and that the mechanism can be described by the pseudo second order kinetics.

## References

- Peterlene W.S., Winkler-Hechenleitner A.A., E.A.G. Pineda, *Bioresour. Technol.* 68 (1999) 95.
- Dakiky M., Khamis M., Manassra A., Mer'eb M., *Adv. Environ. Res.* 6 (2002) 533.
- Wan Ngah W.S., Endud C.S., Mayanar R., *eact. Funct. Polym.* 50 (2002) 181.
- Barrera H., Urena-Nunez F., Bilyeu B., Barrera-Diaz C., *Journal of Hazardous Materials.* 136 (2006) 846.
- Crist R.H., Martin R.J., Crist D.R., *Environ. Sci. Technol.* 33 (1999) 2252.
- Malkoc E., Nuhoglu Y., *Chem. Eng. Sci.* 61 (2006) 4363.
- Berthelin J., BOURRELIER., *Académie des sciences. Technique et documentation,* (1998).
- Nuhoglu Y., Oguz E., *Process. Biochem.* 38 (2003) 1627.
- Rao C. S., *Wiley Eastern Limited.* (1992) 313.
- Hamdaoui O., Naffrechoux., *Lebanese Science Journal.* 06 (2005) 59.
- Crini G., Badot P. M., *Presses universitaires de Franche-Comté, Besançon,* (2007) 352.
- Koriche Y., Hadj Sadoke A., *Revue des Energies Renouvelables.* Alger, 157 (2008) 157.
- Gaballah I., Kibertus G., *J. Geochem. Explor.* 62 (1998) 241.
- Limousin G., Gaudet J. P., Charlet L., Szenkenect S., Barthes V., krimissa M. *measurement-Applied Geochemistry.* 22 (2007) 249.
- Malkoc, E., *Journal of Hazardous Materials.* 137 (2006) 899.
- Hanif M.A., Nadeem R., Bhatti H.N., Ahmed N.R., Ansari T.M., *Journal of Hazardous Materials.* 139 (2007) 345.
- Dundar, M., Nuhoglu, C., Nuhoglu, Y., *Journal of Hazardous Materials.* 151 (2008) 186.
- Hameed B.H., *Journal of Hazardous Materials.* 154 (2008) 204.
- Hamdaoui O., *Journal of Hazardous Materials.* 135 (2006) 264.
- Hinz C., *Goederm.* 99 (2001) 225.
- Maather F.S., Jose R.P., Jaime R.G., Maria D.G., Jorge L., Gardea-Torresdey., *J. Chem. Thermodynamics.* 39 (2007) 488.
- Mehmet E.A., Sukru D., Celalettin O., Karatas M., *Journal of Hazardous Materials.* 141 (2007) 77.
- Hamdaoui O., Naffrechoux E., *Journal of Hazardous Materials.* 147 (2007) 381.
- Wang S., et al., *Journal of colloid and interfacescience.* 284 (2005) 440.
- Gurses A., Dogar C., Yalc in M., Acikyildiz M., Bayrak R. et Karaca S., *Journal of Hazardous Materials.* 131 (2006) 217.

(2015) ; <http://www.jmaterenvironsci.com/>